RESEARCH ARTICLE | SEPTEMBER 24 2024

Explicit and approximate solutions for a classical hyperbolic fragmentation equation using a hybrid projected differential transform method

Nisha Yadav; Zeeshan Ansari ; Randhir Singh ; Ashok Das; Sukhjit Singh; Stefan Heinrich ; Mehakpreet Singh

Physics of Fluids 36, 093343 (2024)
https://doi.org/10.1063/5.0225671

Explicit and approximate solutions for a classical hyperbolic fragmentation equation using a hybrid projected differential transform method

Cite as: Phys. Fluids **36**, 093343 (2024); doi: 10.1063/5.0225671
Submitted: 26 June 2024 · Accepted: 31 August 2024 ·
Published Online: 24 September 2024

Nisha Yadav,[1] Zeeshan Ansari,[2] Randhir Singh,[3,a)] Ashok Das,[4,a)] Sukhjit Singh,[1,a)] Stefan Heinrich,[5,a)] and Mehakpreet Singh[2,a)]

AFFILIATIONS

[1]Department of Mathematics and Computing, Dr. B. R. Ambedkar National Institute of Technology Jalandhar, Punjab, India
[2]Mathematics Applications Consortium for Science and Industry (MACSI), Department of Mathematics and Statistics, University of Limerick, V94 T9PX Limerick, Ireland
[3]Department of Mathematics, Birla Institute of Technology Ranchi, Jharkhand, India
[4]Department of Mathematics and Computing, Indian Institute of Technology (ISM) Dhanbad, Jharkhand 826004, India
[5]Institute of Solids Process Engineering and Particle Technology, Hamburg University of Technology, Denickestraße 15, 21073 Hamburg, Germany

[a)]**Authors to whom correspondence should be addressed:** randhirsingh@bitmesra.ac.in; ashokdas@iitism.ac.in; kundalss@nitj.ac.in; stefan.heinrich@tuhh.de; and Mehakpreet.Singh@ul.ie

ABSTRACT

Population balance equations are widely used to study the evolution of aerosols, colloids, liquid–liquid dispersion, raindrop fragmentation, and pharmaceutical granulation. However, these equations are difficult to solve due to the complexity of the kernel structures and initial conditions. The hyperbolic fragmentation equation, in particular, is further complicated by the inclusion of double integrals. These challenges hinder the analytical solutions of number density functions for basic kernel classes with exponential initial distributions. To address these issues, this study introduces a new approach combining the projected differential transform method with Laplace transform and Padé approximants to solve the hyperbolic fragmentation equation. This method aims to provide accurate and efficient explicit solutions to this challenging problem. The approach's applicability is demonstrated through rigorous mathematical derivation and convergence analysis using the Banach contraction principle. Additionally, several numerical examples illustrate the accuracy and robustness of this new method. For the first time, new analytical solutions for number density functions are presented for various fragmentation kernels with gamma and other initial distributions. This method significantly enhances solution quality over extended periods using fewer terms in the truncated series. The solutions are compared and verified against the finite volume method and the homotopy perturbation method, showing that the coupled approach not only estimates number density functions accurately but also captures integral moments with high precision. This research advances computational methods for particle breakage phenomena, offering potential applications in various industrial processes and scientific disciplines.

I. INTRODUCTION

Particle breakage (or fragmentation), a ubiquitous phenomenon in various fields, encompasses the fragmentation of particles into smaller fragments due to mechanical, chemical, or thermal actions. These particles can be solid granules, liquid droplets, or air bubbles.[1–3] Understanding particle breakage mechanisms and predicting particle size distributions are crucial in numerous applications across various industries and disciplines.[4] In mineral processing, particle breakage is pivotal in processes such as grinding, crushing, and milling, where ores are fragmented to liberate valuable minerals from gangue material.[5–7] The efficiency of mineral extraction and subsequent separation processes, such as flotation, heavily relies on the particle size distribution of the ore feed. Similarly, in pharmaceutical manufacturing, the particle size distribution significantly impacts the performance of drug

formulations. Comminution of active pharmaceutical ingredients is essential to achieve the desired particle size for effective drug delivery.[8–10] Moreover, particle breakage is relevant in various other industrial processes, including fluidized-bed combustion,[11,12] foods and beverages,[13] and liquid droplet dispersion.[14] Achieving the desired particle size distribution is critical for product performance and manufacturing ability across these industries.

Therefore, researchers have shown significant interest in exploring various models related to the particle breakage process. Breakage represents the reverse process of aggregation, wherein two or more particles are generated from the disintegration of a larger particle. Breakage categorized under population balance equations (PBEs) provide a robust mathematical framework for describing the evolution of particle size distributions in systems undergoing fragmentation. These equations are derived based on the fundamental principles of conserving the total mass of the system. While multiple breakage events can occur in real-world scenarios, focusing on modeling breakage in industrial processes offers numerous advantages, including process optimization, product quality control, efficient resource utilization, and the design and maintenance of equipment. The PBE for tracking the temporal evolution of the number density function $\eta(\nu, t)$ varied due to the fragmentation process is provided as follows:[15]

$$\frac{\partial \eta(\nu,t)}{\partial t} = \int_0^\infty B(\nu,y)\,\eta(\nu+y,t)\,\mathrm{d}y - \frac{1}{2}\int_0^\nu B(\nu-y,y)\,\eta(\nu,t)\,\mathrm{d}y, \tag{1}$$

with the initial number density function

$$\eta(\nu,0) = \eta_0(\nu) \geq 0 \quad \text{for all} \quad \nu > 0. \tag{2}$$

The PBE (1) balances the temporal rate of change in the number density distribution by accounting for the subtraction of the frequency of breakage events of particles with size ν from the accumulation rate of particles with size ν due to the breakage of larger particles. The function $B(\nu, y)$, known as the binary fragmentation kernel, quantifies the rate at which particles with size $(\nu + y)$ split into two progeny particles with sizes ν and y. It is important to note that, by assumption, the binary fragmentation kernel $B(\nu, y)$ is considered a non-negative symmetric function of its arguments and equals zero if either ν or y is zero.

The breakage PBE (1) contains two integral terms on the number density function, rendering it challenging to solve and obtain accurate results for physically relevant breakage kernels. Furthermore, the conservation of mass (or volume) is a fundamental property of particle breakage processes. Consequently, many researchers opt for an alternative conservative form of the PBE (1). This alternative formulation not only preserves the volume conservation property but also contains only one integral term on the number density function,[16]

$$\frac{\partial \nu\eta(\nu,t)}{\partial t} = \frac{\partial}{\partial \nu}\left(\int_0^\nu \int_{\nu-y}^\infty y\,B(y,z)\,\eta(y+z,t)\,dz\,dy\right). \tag{3}$$

This study focuses on the development of a new hybrid semi-analytical technique capable of accurately solving the breakage PBE (3) over larger time domains corresponding to a wide range of fragmentation kernels and initial conditions.

For a better understanding of the process within a dynamical system, additional information regarding essential properties, such as the total volume and total number of particles, is imperative. These properties, referred to as integral moments, are obtained through the following expression:

$$\mu_l(t) = \int_0^\infty \nu^l\,\eta(\nu,t)\,d\nu \quad \text{for} \quad l = 0, 1, 2, \ldots. \tag{4}$$

These integral moments play a crucial role and are of practical interest in capturing various properties such as the total volume and total number of particles in the system.[17–20] For example, the zeroth order moment μ_0 determines the total number of particles, while the first order moment μ_1 represents their total volume in the system. Volume conservation is expressed by the following condition:

$$\int_0^\infty \nu\,\eta(\nu,t)\,d\nu = \int_0^\infty \nu\,\eta(\nu,0)\,d\nu, \tag{5}$$

which states that the volume of the population at any time t is equal to that at time $t = 0$. It is worth noting that the hyperbolic fragmentation PBE (3) is primarily expressed in the volume conservative form, ensuring highly accurate time evolution of particle mass.

A. Literature review and motivation

The complex structure and diverse applications, including breakup in bubble columns and depolymerization, of the hyperbolic Eq. (3), have motivated numerous researchers to investigate this PBE. The complexity of Eq. (3) is contingent upon the fragmentation kernel and the presence of double dependent integrals, with analytical solutions available only for certain cases.[15,21] To address this challenge, various numerical approaches have been explored, such as methods of moments,[22,23] sectional discretizations,[24–30] and population dynamics algorithms.[31–34] Additionally, analytical[35–38] and semi-analytical approaches[39–43] have been employed to solve different models of the PBE. Despite the wealth of research, analytical solutions for Eq. (3) are primarily established for simple structured kernels with exponential and Dirac delta initial distributions. More recently, Kushwah and Saha[15] demonstrated the application of the homotopy perturbation method to Eq. (3), obtaining series solutions for various fragmentation kernels with initial distributions $e^{-\nu}$ and $e^{-\nu}/\nu$. However, it is noteworthy that the solution accuracy of this method is constrained to short time intervals and exhibits peculiar behavior over longer intervals.

On the other hand, in recent decades, considerable interest has emerged in solving various linear and nonlinear problems using the differential transform method (DTM). Zhou[44] introduced the differential transform method in 1986 and applied it to solve nonlinear problems in electrical circuits. A significant advantage of this approach is its direct applicability to nonlinear problems without the need for discretization, linearization, or perturbation. As a semi-analytical method, the DTM uniquely formulates Taylor series solutions, iteratively generating them unlike the ordinary high-order Taylor series method that involves symbolic computation. This feature minimizes computational work compared to the computationally intensive Taylor series method. DTM has proven to be a simple and effective approach for solving a variety of problems, including two-point boundary-value problems,[45] nonlinear biochemical reaction models,[46] differential-algebraic equations,[47] and Schrödinger equations,[48] among others.

Furthermore, researchers have enhanced the DTM for solving fractional differential and integrodifferential equations.[49–51] Jang[52]

noted that the ordinary differential transform method consumes significant computational time when addressing multidimensional problems. To overcome this challenge, Jang proposed the modified DTM, known as the projected differential transform method (PDTM), for solving both linear and nonlinear multidimensional problems. In a recent study by Akinfe and Loyinmi,[53] PDTM with Elzaki transform was employed to solve the renowned Schrödinger equation prevalent in field theory, waves, and quantum physics.

The major challenge associated with DTM and its modifications lies in obtaining inaccurate approximate solutions over larger intervals. To overcome this issue, some researchers have combined Padé approximants and Laplace transformation with PDTM to extend the series solutions of PDTM over larger intervals.[54,55] This modification of PDTM has demonstrated increased efficiency in various applications.[56,57] This motivates the application of the coupled PDTM and Padé approximant to address the hyperbolic breakage PBE (3). In the majority of cases examined in this study, we derive explicit or closed-form solutions for number density functions using Laplace transformation with PDTM. Nonetheless, in certain instances, capturing closed-form solutions proves exceedingly challenging due to the complex nature of the breakage kernel. Hence, we delve into the implementation of Padé approximants on the series solutions estimated through Laplace transformation with PDTM, as detailed in Sec. IV B.

The remaining content of the paper is structured as follows. Section II A provides the basic definition and properties of the projected differential transform method. In Sec. II, we present the mathematical derivation and convergence analysis of the Laplace projected differential transform method applied to the hyperbolic fragmentation equation. Section III introduces the fundamental concepts of Padé approximants. We present numerical examples and comparisons with the homotopy perturbation method (HPM) in Sec. IV. Finally, Sec. V of the paper is use to conclude and summarize the outcomes of current study.

II. LAPLACE TRANSFORMATION WITH PDTM FOR HYPERBOLIC FRAGMENTATION EQUATION

Before deriving the mathematical expression of the PDTM using the Laplace transform, let us first present the basic definition and some important properties of the PDTM.

A. Definitions and basics properties

Definition 1. *Let $g(y_1, y_2, \ldots, y_n) \in \mathbb{R}^n$, then its projected differential transform with respect to y_n at y_{n0} is defined as*

$$G(y_1, y_2, \ldots, y_{n-1}, j) = \frac{1}{j!}\left[\frac{\partial^j}{\partial y_n^j} g(y_1, y_2, \ldots, y_n)\right]_{y_n = y_{n0}}, \tag{6}$$

while the inverse PDT of Eq. (6) *with respect to y_n at y_{n0} is given by*

$$g(y_1, y_2, \ldots, y_n) = \sum_{j=0}^{\infty} G(y_1, y_2, \ldots, y_{n-1}, j)(y_n - y_{n0})^j. \tag{7}$$

It can be seen that (7) represents the Taylor series of $g(y_1, y_2, \ldots, y_n)$ at $y_n = y_{n0}$, combining (6) and (7), the function $g(y_1, y_2, \ldots, y_n)$ can be expressed as

$$g(y_1, y_2, \ldots, y_n) = \sum_{j=0}^{\infty} \frac{1}{j!}\left[\frac{\partial^j}{\partial y_n^j} g(y_1, y_2, \ldots, y_n)\right]_{y_n = y_{n0}} (y_n - y_{n0})^j. \tag{8}$$

Some basic properties obtained by the above-mentioned definition are given below. Let $f(y_1, y_2, \ldots, y_n)$, $g(y_1, y_2, \ldots, y_n)$, and $h(y_1, y_2, \ldots, y_n)$ be functions in $\mathbb{R}^n$ and $F(y_1, y_2, \ldots, y_{n-1}, j)$ $G(y_1, y_2, \ldots, y_{n-1}, j)$, $H(y_1, y_2, \ldots, y_{n-1}, j)$ are transformed functions of f, g, and h, respectively.

1. If $f(y_1, y_2, \ldots, y_n) = \alpha g(y_1, y_2, \ldots, y_n) + \beta h(y_1, y_2, \ldots, y_n)$, then $F(y_1, y_2, \ldots, y_{n-1}, j) = \alpha G(y_1, y_2, \ldots, y_{n-1}, j) + \beta H(y_1, y_2, \ldots, y_{n-1}, j)$, where α and β are any two real constants.
2. If $f(y_1, y_2, \ldots, y_n) = g_1(y_1, y_2, \ldots, y_n)\, g_2(y_1, y_2, \ldots, y_n) \ldots g_n(y_1, y_2, \ldots, y_n)$, then $F(y_1, y_2, \ldots, y_{n-1}, j) = \sum_{j_{n-1}=0}^{j} \sum_{j_{n-2}=0}^{j_{n-1}} \ldots \sum_{j_1=0}^{j_2} G_1(y_1, y_2, \ldots, y_{n-1}, j_1)\, G_2(y_1, y_2, \ldots, y_{n-1}, j_2 - j_1) \ldots G_n(y_1, y_2, \ldots, y_{n-1}, j_n - j_{n-1})$.
3. If $f(y_1, y_2, \ldots, y_n) = \frac{\partial^n g(y_1, y_2, \ldots, y_n)}{\partial y_n^n}$, then $F(y_1, y_2, \ldots, y_{n-1}, j) = \frac{j+n}{j!} G(y_1, y_2, \ldots, y_{n-1}, j+n)$.

B. Mathematical formulation of the proposed approach

In this subsection, the PDTM with Laplace transformation (LPDTM) is employed on a classical hyperbolic fragmentation Eq. (3) that involves double integral term and establish the convergence analysis using the Banach contraction principle. On applying the Laplace transform (LT) of Eq. (3) and using the properties of LT, we get

$$\mathcal{L}[\eta(\nu, t)] = \frac{\eta_0(\nu)}{s} + \frac{1}{s}\mathcal{L}\left[\frac{1}{\nu}\frac{\partial}{\partial \nu}\left(\int_0^{\nu}\int_{\nu-y}^{\infty} yB(y, z)\eta(y+z, t)\, dz\, dy\right)\right], \tag{9}$$

where $\mathcal{L}$ represents the Laplace transform operator. Using the inverse Laplace transformation to Eq. (9) leads to

$$\eta(\nu, t) = \eta(\nu, 0) + \mathcal{L}^{-1}\left\{\frac{1}{s}\mathcal{L}\left[\frac{1}{\nu}\frac{\partial}{\partial \nu}\left(\int_0^{\nu}\int_{\nu-y}^{\infty} yB(y, z)\eta(y+z, t)\, dz\, dy\right)\right]\right\}. \tag{10}$$

According to the PDTM, solution $\eta(\nu, t)$ can be written in the series form as

$$\eta(\nu, t) = \sum_{k=0}^{\infty} \eta_k(\nu, t). \tag{11}$$

The iterative algorithm to calculate the components $\eta_k's$, after putting (11) in Eq. (10) and comparing the coefficients, is given as

$$\eta_{k+1}(\nu, t) = \mathcal{L}^{-1}\left\{\frac{1}{s}\mathcal{L}\left[\frac{1}{\nu}\frac{\partial}{\partial \nu}\left(\int_0^{\nu}\int_{\nu-y}^{\infty} yB(y, z)\eta_k(y+z, t)\, dz\, dy\right)\right]\right\}, \tag{12}$$

with $\eta_0(\nu, t) = \eta(\nu, 0)$. After determining the solution components $\eta_k(\nu, t)$, the n-terms series solution is given by

$$\Psi_n(\nu, t) = \sum_{k=0}^{n} \eta_k(\nu, t). \tag{13}$$

C. Convergence analysis

Next, we discuss the convergence analysis of the proposed method for solving the hyperbolic fragmentation PBE (3). To facilitate this discussion, let

$$\mathcal{B} = \{\eta : [0,\infty) \times [0,T] \to [0,\infty) : \eta \text{ is continuous}\} \tag{14}$$

be a Banach space (see A for proof) with the following norm as

$$||\eta||_{\mathcal{B}} = \sup_{t\in[0,T]} \int_0^\infty (1+\nu)|\eta|\, d\nu < \infty. \tag{15}$$

Theorem 2.1. *Assume that*

$$\mathcal{S}_k = \eta_1 + \eta_2 + \cdots + \eta_k \tag{16}$$

is a sequence with $\mathcal{S}_0 = 0$ *and satisfying the following relation*:

$$\mathcal{S}_{k+1} = \mathcal{L}^{-1}\left\{\frac{1}{s}\mathcal{L}\left[\frac{1}{\nu}\frac{\partial}{\partial\nu}\left(\int_0^\nu\int_{\nu-y}^\infty yB(y,z)(\mathcal{S}_k+\eta_0)\,dz\,dy\right)\right]\right\}, \quad k = 0,1,2,\ldots, \tag{17}$$

then, determining the above-mentioned sequence S_k is equivalent to the kth-order series solution of Eq. (3) using LPDTM.

Proof. To prove this theorem, we will use the strong induction theorem. First, we will validate the result for $k = 0, 1$. Later, it will be considered that the hypothesis holds for k and thus will be proved for $k+1$.

For $k = 0$, Eq. (17) becomes

$$\begin{aligned}\mathcal{S}_1 &= \mathcal{L}^{-1}\left\{\frac{1}{s}\mathcal{L}\left[\frac{1}{\nu}\frac{\partial}{\partial\nu}\left(\int_0^\nu\int_{\nu-y}^\infty yB(y,z)(\mathcal{S}_0+\eta_0)\,dz\,dy\right)\right]\right\}\\ &= \mathcal{L}^{-1}\left\{\frac{1}{s}\mathcal{L}\left[\frac{1}{\nu}\frac{\partial}{\partial\nu}\left(\int_0^\nu\int_{\nu-y}^\infty yB(y,z)(\eta_0)\,dz\,dy\right)\right]\right\}.\end{aligned}$$

From Eq. (16), $\mathcal{S}_1 = \eta_1$. Therefore,

$$\eta_1 = \mathcal{L}^{-1}\left\{\frac{1}{s}\mathcal{L}\left[\frac{1}{\nu}\frac{\partial}{\partial\nu}\left(\int_0^\nu\int_{\nu-y}^\infty yB(y,z)(\eta_0)\,dz\,dy\right)\right]\right\}, \tag{18}$$

which is equivalent to η_1 derived using the LPDTM (12). For $k = 1$, Eq. (17) becomes

$$\begin{aligned}\mathcal{S}_2 &= \mathcal{L}^{-1}\left\{\frac{1}{s}\mathcal{L}\left[\frac{1}{\nu}\frac{\partial}{\partial\nu}\left(\int_0^\nu\int_{\nu-y}^\infty yB(y,z)(\mathcal{S}_1+\eta_0)\,dz\,dy\right)\right]\right\}\\ &= \mathcal{L}^{-1}\left\{\frac{1}{s}\mathcal{L}\left[\frac{1}{\nu}\frac{\partial}{\partial\nu}\left(\int_0^\nu\int_{\nu-y}^\infty yB(y,z)(\eta_1+\eta_0)\,dz\,dy\right)\right]\right\}\\ &= \eta_1 + \mathcal{L}^{-1}\left\{\frac{1}{s}\mathcal{L}\left[\frac{1}{\nu}\frac{\partial}{\partial\nu}\left(\int_0^\nu\int_{\nu-y}^\infty yB(y,z)(\mathcal{S}_1)\,dz\,dy\right)\right]\right\},\end{aligned}$$

and from Eq. (16), $\mathcal{S}_2 = \eta_1 + \eta_2$. Therefore,

$$\eta_2 = \mathcal{L}^{-1}\left\{\frac{1}{s}\mathcal{L}\left[\frac{1}{\nu}\frac{\partial}{\partial\nu}\left(\int_0^\nu\int_{\nu-y}^\infty yB(y,z)(\mathcal{S}_1)\,dz\,dy\right)\right]\right\}, \tag{19}$$

which is again the same as η_2 derived from the LPDTM (12). Moreover, it is assumed that

$$\eta_{n+1} = \mathcal{L}^{-1}\left\{\frac{1}{s}\mathcal{L}\left[\frac{1}{\nu}\frac{\partial}{\partial\nu}\left(\int_0^\nu\int_{\nu-y}^\infty yB(y,z)(\eta_n)\,dz\,dy\right)\right]\right\}, \quad n = 1,2,\ldots,k-1. \tag{20}$$

Consider

$$\begin{aligned}\mathcal{S}_{k+1} &= \mathcal{L}^{-1}\left\{\frac{1}{s}\mathcal{L}\left[\frac{1}{\nu}\frac{\partial}{\partial\nu}\left(\int_0^\nu\int_{\nu-y}^\infty yB(y,z)(\mathcal{S}_k+\eta_0)\,dz\,dy\right)\right]\right\}\\ &= \mathcal{L}^{-1}\left\{\frac{1}{s}\mathcal{L}\left[\frac{1}{\nu}\frac{\partial}{\partial\nu}\left(\int_0^\nu\int_{\nu-y}^\infty yB(y,z)\left(\sum_{n=0}^{k}\eta_k\right)dz\,dy\right)\right]\right\}\\ &= \sum_{n=1}^{k} + \mathcal{L}^{-1}\left\{\frac{1}{s}\mathcal{L}\left[\frac{1}{\nu}\frac{\partial}{\partial\nu}\left(\int_0^\nu\int_{\nu-y}^\infty yB(y,z)(\eta_k)\,dz\,dy\right)\right]\right\}.\end{aligned}$$

From Eq. (16), we obtain

$$\eta_{k+1} = \mathcal{L}^{-1}\left\{\frac{1}{s}\mathcal{L}\left[\frac{1}{\nu}\frac{\partial}{\partial\nu}\left(\int_0^\nu\int_{\nu-y}^\infty yB(y,z)(\eta_k)\,dz\,dy\right)\right]\right\}, \tag{21}$$

which is the same as the iterative scheme (12) obtained from the LPDTM. □

Next, we will show that $\mathcal{S}_k$ is a Cauchy sequence in Banach space $\mathcal{B}$ and hence converges.

Theorem 2.2. *If* $\lambda \in [0,1]$ *such that* $||\eta_k||_{\mathcal{B}} \le \lambda||\eta_{k-1}||_{\mathcal{B}}$ *for all* $k \in \mathbb{N}$, *then the series* $\sum_{k=1}^{\infty}\eta_k$ *converges to some* $\mathcal{S} \in \mathcal{B}$, *where* η_k *are obtained by iterative scheme (12) and* $\mathcal{S}$ *satisfies*

$$\mathcal{S} = \mathcal{L}^{-1}\left\{\frac{1}{s}\mathcal{L}\left[\frac{1}{\nu}\frac{\partial}{\partial\nu}\left(\int_0^\nu\int_{\nu-y}^\infty yB(y,z)(\mathcal{S}+\eta_0)\,dz\,dy\right)\right]\right\}. \tag{22}$$

Proof. Let there exists $\lambda \in [0,1)$ such that $||\eta_k||_{\mathcal{B}} \le \lambda||\eta_{k-1}||_{\mathcal{B}}$, for all $k \in \mathbb{N}$, then

$$||\mathcal{S}_{k+1} - \mathcal{S}_k||_{\mathcal{B}} = ||\eta_{k+1}||_{\mathcal{B}} \le \lambda||\eta_k||_{\mathcal{B}} \le \ldots \le \lambda^{k+1}||\eta_0||_{\mathcal{B}}. \tag{23}$$

Now for any $k, l \in \mathbb{N}$, with $k \ge l$, we have

$$\begin{aligned}&||\mathcal{S}_k - \mathcal{S}_l||_{\mathcal{B}}\\ &= ||(\mathcal{S}_k - \mathcal{S}_{k-1} + \mathcal{S}_{k-1} - \mathcal{S}_{k-2} + \cdots + \mathcal{S}_{l+1} - \mathcal{S}_l)||_{\mathcal{B}}\\ &\le ||\mathcal{S}_k - \mathcal{S}_{k-1}||_{\mathcal{B}} + ||\mathcal{S}_{k-1} - \mathcal{S}_{k-2}||_{\mathcal{B}} + \cdots + ||\mathcal{S}_{l+1} - \mathcal{S}_l||_{\mathcal{B}}\\ &\le (\lambda^{l+1} + \cdots + \lambda^k + \cdots)||\eta_0||_{\mathcal{B}}\\ &\le \lambda^{l+1}(1 + \lambda + \lambda^2 + \cdots + \lambda^k + \cdots)||\eta_0||_{\mathcal{B}}\\ &\le \frac{\lambda^{l+1}}{1-\lambda}||\eta_0||_{\mathcal{B}}.\end{aligned}$$

Therefore, $\lim_{k,l\to\infty}||\mathcal{S}_k - \mathcal{S}_l||_{\mathcal{B}} = 0$. Thus, $\mathcal{S}_k$ is Cauchy in $\mathcal{B}$ and hence converges. Therefore, there exists $\mathcal{S} \in \mathcal{B}$ such that $\lim_{k\to\infty}\mathcal{S}_k = \sum_{k=1}^{\infty}\eta_k = \mathcal{S}$. Now

$$\begin{aligned}\mathcal{S} &= \lim_{k\to\infty} \mathcal{S}_{k+1} \\ &= \mathcal{L}^{-1} \lim_{k\to\infty} \left\{ \frac{1}{s} \mathcal{L} \left[\frac{1}{\nu} \frac{\partial}{\partial \nu} \left(\int_0^{\nu} \int_{\nu-y}^{\infty} yB(y,z)(\mathcal{S}_k + \eta_0)\, dz\, dy \right) \right] \right\} \\ &= \mathcal{L}^{-1} \left\{ \frac{1}{s} \mathcal{L} \left[\frac{1}{\nu} \frac{\partial}{\partial \nu} \left(\int_0^{\nu} \int_{\nu-y}^{\infty} yB(y,z) \left(\lim_{k\to\infty} \sum_{i=0}^{k} \eta_i \right) dz\, dy \right) \right] \right\} \\ &= \mathcal{L}^{-1} \left\{ \frac{1}{s} \mathcal{L} \left[\frac{1}{\nu} \frac{\partial}{\partial \nu} \left(\int_0^{\nu} \int_{\nu-y}^{\infty} yB(y,z) \left(\sum_{i=0}^{\infty} \eta_i \right) dz\, dy \right) \right] \right\} \\ &= \mathcal{L}^{-1} \left\{ \frac{1}{s} \mathcal{L} \left[\frac{1}{\nu} \frac{\partial}{\partial \nu} \left(\int_0^{\nu} \int_{\nu-y}^{\infty} yB(y,z)(\mathcal{S} + \eta_0)\, dz\, dy \right) \right] \right\}.\end{aligned}$$

Lemma 2.1. *Equation (22) is equivalent to the hyperbolic fragmentation Eq. (3).*

Proof. From Eq. (22), we have

$$\mathcal{S} = \mathcal{L}^{-1} \left\{ \frac{1}{s} \mathcal{L} \left[\frac{1}{\nu} \frac{\partial}{\partial \nu} \left(\int_0^{\nu} \int_{\nu-y}^{\infty} yB(y,z)(\mathcal{S} + \eta_0)\, dz\, dy \right) \right] \right\}. \tag{24}$$

Using the property of Laplace transformation,

$$\begin{aligned}\mathcal{S} &= \int_0^t \frac{1}{\nu} \frac{\partial}{\partial \nu} \left(\int_0^{\nu} \int_{\nu-y}^{\infty} yB(y,z)(\mathcal{S} + \eta_0)(\nu,\tau)\, dz\, dy \right) d\tau, \\ \frac{\partial \mathcal{S}}{\partial t} &= \frac{1}{\nu} \frac{\partial}{\partial \nu} \left(\int_0^{\nu} \int_{\nu-y}^{\infty} yB(y,z)(\mathcal{S} + \eta_0)(\nu,t)\, dz\, dy \right).\end{aligned} \tag{25}$$

Let $\eta = \mathcal{S} + \eta_0 = \sum_{k=0}^{\infty} \eta_k$, Eq. (22) gives Eq. (3). Therefore, the solution of Eq. (22) is same as the solution of Eq. (3). □

III. THE PADÉ APPROXIMANTS

In this section, we discuss how to construct the Padé approximant of the series solution derived from the LPDTM. Let the truncated series solution (13) can be written as

$$\Psi_k(\nu,t) = \sum_{l=0}^{r+s=k} p_l(\nu) t^l. \tag{26}$$

Then, the $[r,s]$ order Padé approximant (see Refs. 58 and 59) of series solution $\Psi_k(\nu,t)$ is defined by the ratio of two polynomials of degree r and s, respectively, that is,

$$\Psi_k(\nu,t) \simeq [r,s]_{\Psi_k} = \frac{a_0(\nu) + a_1(\nu)t + \cdots + a_r(\nu)t^r}{1 + c_1(\nu)t + \cdots + c_s(\nu)t^s} = \frac{\mathcal{A}(\nu,t)}{\mathcal{C}(\nu,t)}. \tag{27}$$

Here, the normalization condition is used, i.e., $\mathcal{C}(\nu,0) = 1$, and it is ensured that there are no common factors between $\mathcal{A}(\nu,t)$ and $\mathcal{C}(\nu,t)$. This means that $c_0(\nu) = 1$ and $\Psi_k(\nu,t)$ equals the $[r,s]$ approximant through $r+s+1$ terms. The unknown coefficients $a_r's$ and $c_s's$ of the polynomials $\mathcal{A}(\nu,t)$ and $\mathcal{C}(\nu,t)$ are determined by the coefficients of the function $\Psi_k(\nu,t)$. Therefore, Eqs. (26) and (27) yield

$$\begin{aligned}a_0 + a_1 t + \cdots + a_r t^r = (1 + c_1 t + \cdots + c_s t^s) \\ \times (p_0 + p_1 t + \cdots + p_{r+s} t^{r+s}).\end{aligned} \tag{28}$$

From Eq. (28), we obtain the following system of equations:

$$\begin{aligned} p_{r+1} + p_r c_1 + \cdots + p_{p-s+1} c_s &= 0, \\ p_{r+2} + p_{r+1} c_1 + \cdots + p_{p-s+2} c_s &= 0, \\ &\vdots \\ p_{r+b} + p_{r+b-1} c_1 + \cdots + p_r c_s &= 0, \end{aligned} \tag{29}$$

$$\begin{aligned} p_0 &= a_0, \\ p_1 + p_0 c_1 &= a_1, \\ p_2 + p_1 c_1 + p_0 c_2 &= a_2, \\ &\vdots \\ p_r + p_{r-1} c_1 + \cdots + p_0 c_r &= a_r. \end{aligned} \tag{30}$$

Thus, the coefficients of $\mathcal{A}(\nu,t)$ and $\mathcal{B}(\nu,t)$ are evaluated by solving the system of equations defined in Eqs. (29) and (30). The primary advantage of constructing $[r,s]$ Padé approximants is that it simply requires algebraic operations, with each choice of r and s yielding an approximant. However, the key challenge lies in identifying the order of the Padé approximant that leads to the best approximation. This necessitates the use of criteria dependent on the behavior of the solution. We select the smallest order, $[r,s]$, which matches the exact solution very accurately. In cases where an exact solution is unavailable, we compare the behavior of the Padé approximant with the available finite volume scheme (FVM)[60] solution to determine the order that yields a better approximation. It is noteworthy that the *pade* inbuilt command in MATLAB is utilized for finding the approximant. All simulations are conducted on an Intel Core i3-6006U CPU operating at 2.00 GHz with 4.00 GB of RAM using MATLAB R2019a software.

IV. NUMERICAL RESULTS

In this section, five test cases are considered, encompassing various combinations of fragmentation kernels and initial conditions, to illustrate the applicability of coupled approach based on the Laplace projected differential transform and Padé approximant (LPDTM-PA). It is noteworthy that, owing to the availability of analytical (exact) solutions[21] for the first two problems, the verification of the proposed method is conducted in terms of number density and its integral moments. Additionally, we have determined the errors in the number density function for these kernels. The quantitative relative error is estimated using the following expression:

$$\text{Error} = \left| \frac{\eta(\nu,t) - \eta_{app}(\nu,t)}{\eta(\nu,t)} \right|, \tag{31}$$

where $\eta(\nu,t)$ represents the exact solution and $\eta_{\text{app}}(\nu,t)$ denotes the approximate solution obtained from LPDTM-PA. However, no analytical solutions are available for any type of kernels with the gamma distribution. Therefore, to assess the accuracy of the proposed approach, new closed form series solutions are obtained and validation is done against the existing finite volume scheme (FVM).[60] Note that, throughout all computations, ν and t are treated as dimensionless parameters and can be obtained by dividing with $\nu = 1$ and $t = 1$, respectively.

A. Verification with existing analytical solutions

In this subsection, the solutions for the number density $\eta(\nu,t)$ with fragmentation kernels $B(\nu,y) = 2$, and $B(\nu,y) = 2(\nu+y)$ corresponding to an exponential initial distribution $\eta(\nu,0) = e^{-\nu}$ are

derived and compared against the exact solutions. Moreover, the accuracy is also tested against the recently developed homotopy perturbation method (HPM).[15]

1. $B(\nu, y) = 2$ with an initial distribution $\eta(\nu, 0) = e^{-\nu}$

The analytical solution for this case with an exponential initial condition $\eta(\nu, 0) = e^{-\nu}$ is established by Ziff and McGrady[21] as follows:

$$\eta(\nu, t) = e^{-(1+t)\nu}(1+t)^2. \tag{32}$$

Using the recursive scheme (12), we obtain

$$\begin{aligned}
\eta_0(\nu, t) &= e^{-\nu}, \\
\eta_1(\nu, t) &= e^{-\nu}(\nu - 2)\, t, \\
\eta_2(\nu, t) &= \frac{e^{-\nu}\,(\nu^2 - 4\,\nu + 2)\, t^2}{2}, \\
\eta_3(\nu, t) &= -\frac{\nu\, e^{-\nu}\,(\nu^2 - 6\,\nu + 6)\, t^3}{6}, \\
&\vdots \\
\eta_k(\nu, t) &= \frac{(-1)^k t^k \nu^{k-2} e^{-\nu}(\nu^2 - 2k\nu + k(k-1))}{k!}.
\end{aligned}$$

Therefore, the truncated series solution (TSS) consisting of n terms can be obtained as follows:

$$\Psi_n(\nu, t) = \sum_{k=0}^{n} \frac{(-1)^k t^k \nu^{k-2} e^{-\nu}(\nu^2 - 2k\nu + k(k-1))}{k!}. \tag{33}$$

By letting $n \to \infty$ in Eq. (33), we can obtain the closed-form solution as provided in Ref. 21,

$$\begin{aligned}
\eta(\nu, t) &= \sum_{k=0}^{\infty} \frac{(-1)^k t^k \nu^{k-2} e^{-\nu}(\nu^2 - 2k\nu + k(k-1))}{k!} \\
&\to e^{-(1+t)\nu}(1+t)^2.
\end{aligned} \tag{34}$$

One can observe that the LPDTM exhibits a tendency to effectively capture the closed-form solution for the breakage kernel $B(\nu, y) = 2$, corresponding to an exponential initial distribution. In numerous instances involving complex structured breakage kernels, finding closed or explicit solutions proves challenging. However, the series solutions derived in such scenarios offer accurate solutions within the small time domain. However, the accuracy can be improved for the long time by using the notion of Padé approximant as discussed in Sec. III. To assess the effectiveness of Padé approximants with the LPDTM solution, we consider the 12-term series solution, which is given as follows:

$$\begin{aligned}
\Psi_{12}(\nu,t) = e^{-\nu} &+ \frac{t^2 e^{-\nu}(\nu^2 - 4\nu + 2)}{2} - t e^{-\nu}(\nu - 2) \\
&+ \frac{t^4 \nu^2 e^{-\nu}(\nu^2 - 8\nu + 12)}{24} - \frac{t^5 \nu^3 e^{-\nu}(\nu^2 - 10\nu + 20)}{120} \\
&+ \frac{t^6 \nu^4 e^{-\nu}(\nu^2 - 12\nu + 30)}{720} - \frac{t^7 \nu^5 e^{-\nu}(\nu^2 - 14\nu + 42)}{5040} \\
&+ \frac{t^8 \nu^6 e^{-\nu}(\nu^2 - 16\nu + 56)}{40\,320} - \frac{t^9 \nu^7 e^{-\nu}(\nu^2 - 18\nu + 72)}{362\,880} \\
&+ \frac{t^{10} \nu^8 e^{-\nu}(\nu^2 - 20\nu + 90)}{3628\,800} - \frac{t^{11} \nu^9 e^{-\nu}(\nu^2 - 22\nu + 110)}{39\,916\,800} \\
&+ \frac{t^{12} \nu^{10} e^{-\nu}(\nu^2 - 24\nu + 132)}{479\,001\,600} - \frac{t^3 \nu e^{-\nu}(\nu^2 - 6\nu + 6)}{6}.
\end{aligned} \tag{35}$$

The above-mentioned series solution exhibits a limited region of convergence with respect to time variable t. It is evident that solution (35) can be expressed in the form (26). Therefore, we approximate (35) using an $[6, 6]$ order Padé approximant to broaden the convergence domain and the solutions are demonstrated by Fig. 1. The resulting approximation is plotted in Fig. 1(a) at $t = 4$. We observe that the number density function and its moments (μ_0 and μ_1) obtained using LPDTM-PA closely match with the exact solution [refer to Fig. 1(b)]. However, both LPDTM and HPM method show large deviation and

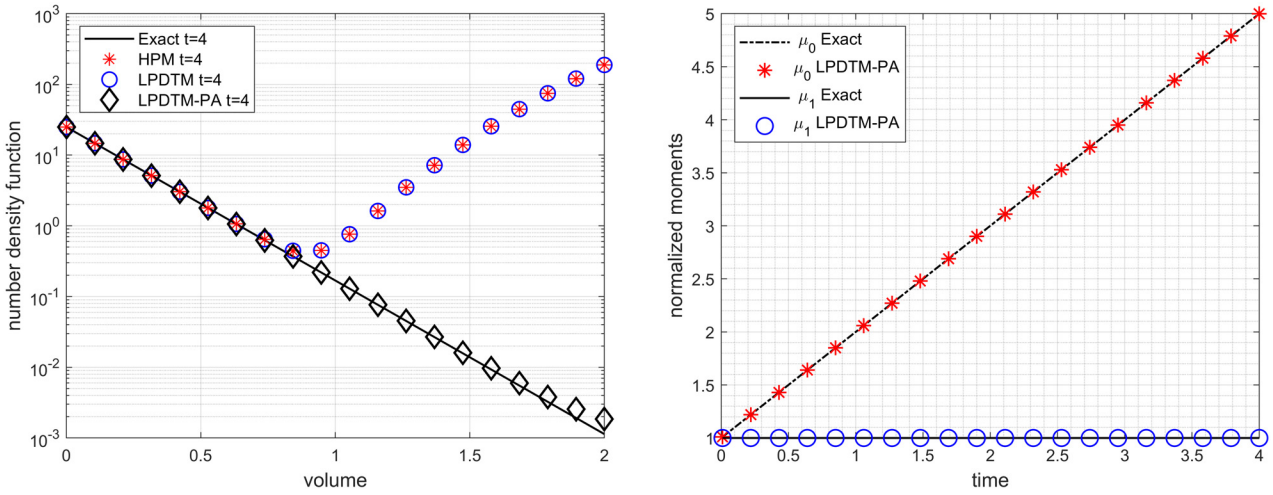

(a) Number density function (b) Normalized moments

FIG. 1. Comparison of series solutions of number density function and moments for $B(\nu, y) = 2$ with IC $\eta(\nu, 0) = e^{-\nu}$: (a) number density function and (b) normalized moments.

TABLE I. Relative errors in the number density function obtained using $B(\nu, y) = 2$ with $\eta(\nu, 0) = e^{-\nu}$.

k	Padé Order	HPM	LPDTM-PA
6	[3,3]	3.1125×10^{-2}	4.9372×10^{-4}
8	[4,4]	1.3279×10^{-2}	2.3171×10^{-5}
10	[5,5]	5.1683×10^{-3}	1.0803×10^{-6}
12	[6,6]	1.7320×10^{-3}	4.9113×10^{-8}

capture solutions only for a short time frame. Furthermore, we analyze the impact of different order Padé approximants on the series solution (35), and the relative errors of HPM and LPDTM-PA are listed in Table I. As expected, the error decreases for both methods as the number of terms in the series solution increases. However, LPDTM-PA outperforms HPM significantly.

2. $B(\nu, y) = 2(\nu + y)$ with an initial distribution $\eta(\nu, 0) = e^{-\nu}$

For this case also, the exact solution provided by Ziff and McGrady[21] is given as follows:

$$\eta(\nu, t) = \sum_{k=0}^{\infty} \frac{(-1)^k t^k \nu^{2k-2} e^{-\nu}(\nu^2 - 2k\nu - 2k)}{k!} \to e^{-(1+t\nu)\nu}(1 + 2t + 2t\nu). \tag{36}$$

Using the expression of LPDTM (12), one can get

$$\begin{aligned}
\eta_0(\nu, t) &= e^{-\nu}, \\
\eta_1(\nu, t) &= e^{-\nu}(-\nu^2 + 2\nu + 2)t, \\
\eta_2(\nu, t) &= -\frac{\nu^2 e^{-\nu}(-\nu^2 + 4\nu + 4)t^2}{2}, \\
\eta_3(\nu, t) &= \frac{\nu^4 e^{-\nu}(-\nu^2 + 6\nu + 6)t^3}{6}, \\
&\vdots \\
\eta_k(\nu, t) &= \frac{(-1)^k t^k \nu^{2k-2} e^{-\nu}(\nu^2 - 2k\nu - 2k)}{k!}.
\end{aligned}$$

Hence, the TSS consisting of n terms is given by

$$\Psi_n(\nu, t) = \sum_{k=0}^{n} \frac{(-1)^k t^k \nu^{2k-2} e^{-\nu}(\nu^2 - 2k\nu - 2k)}{k!}. \tag{37}$$

Taking the limit as $n \to \infty$ allows us to obtain the closed-form solution,

$$\eta(\nu, t) = \sum_{k=0}^{\infty} \frac{(-1)^k t^k \nu^{2k-2} e^{-\nu}(\nu^2 - 2k\nu - 2k)}{k!} \to e^{-(1+t\nu)\nu}(1 + 2t + 2t\nu). \tag{38}$$

Once again, the new approach demonstrates a tendency to capture the closed-form solution for breakage kernel $B(\nu, y) = 2(\nu + y)$ associated with an exponential initial distribution. Similar to the previous case above, the effect of Padé approximant is studied on the 12-term TSS, which is given by

$$\begin{aligned}
\Psi_{12}(\nu, t) &= e^{-\nu} + t e^{-\nu}(-\nu^2 + 2\nu + 2) - \frac{\nu^2 t^2 e^{-\nu}(-\nu^2 + 4\nu + 4)}{2} \\
&+ \frac{\nu^4 t^3 e^{-\nu}(-\nu^2 + 6\nu + 6)}{6} - \frac{\nu^6 t^4 e^{-\nu}(-\nu^2 + 8\nu + 8)}{24} \\
&+ \frac{\nu^8 t^5 e^{-\nu}(-\nu^2 + 10\nu + 10)}{120} - \frac{\nu^{10} t^6 e^{-\nu}(-\nu^2 + 12\nu + 12)}{720} \\
&+ \frac{\nu^{12} t^7 e^{-\nu}(-\nu^2 + 14\nu + 14)}{5040} - \frac{\nu^{14} t^8 e^{-\nu}(-\nu^2 + 16\nu + 16)}{40\,320} \\
&+ \frac{\nu^{16} t^9 e^{-\nu}(-\nu^2 + 18\nu + 18)}{362\,880} - \frac{\nu^{18} t^{10} e^{-\nu}(-\nu^2 + 20\nu + 20)}{3\,628\,800} \\
&+ \frac{\nu^{20} t^{11} e^{-\nu}(-\nu^2 + 22\nu + 22)}{39\,916\,800} - \frac{\nu^{22} t^{12} e^{-\nu}(-\nu^2 + 24\nu + 24)}{479\,001\,600}.
\end{aligned} \tag{39}$$

Similar to the previous case, the 12-term TSS (39) is approximated using an [6, 6] order Padé approximant and plotted in Fig. 2 at time $t = 1.5$. The number density function estimated by LPDTM-PA exhibits a good match with the exact solution, whereas significant deviations are shown by the LPDTM and HPM [see Fig. 2(a)]. In addition, from Fig. 2(b), it is evident that the first-two moments show good agreement with the exact moments. Moreover, the convergence behavior of the number density function with different order Padé approximants is analyzed by estimating the relative errors against the HPM in Table II. It shows that LPDTM-PA approximates the number density function with lesser errors than HPM.

B. Newly derived closed form and series solutions

In this subsection, the new closed form and series solutions are derived for the breakage kernels $B(\nu, y) = 2$, $2(\nu + y)$ and $\frac{2}{\sqrt{\nu+y}}$ with Gamma initial distributions of the forms $4\nu e^{-2\nu}$ and $\nu e^{-\nu}$. It is worth mentioning that no exact solutions are available in the literature for these initial distributions. Therefore, the FVM will be used to assess the accuracy of the new solutions.

1. $B(\nu, y) = 2$ with an initial distribution $\eta(\nu, 0) = 4\nu e^{-2\nu}$

In this case, the fragmentation kernel $B(\nu, y) = 2$ is considered with a gamma initial distribution, that is, $\eta(\nu, 0) = 4\nu e^{-2\nu}$. Due to the non-availability of the exact solution, the validation of the results is accomplished by comparing the number density function and its first-two moments against the FVM results. Using the expression of LPDTM (12), the components of the series are obtained as

$$\begin{aligned}
\eta_0(\nu, t) &= 4\nu e^{-2\nu}, \\
\eta_1(\nu, t) &= 2e^{-2\nu}(-2\nu^2 + 2\nu + 1)t, \\
\eta_2(\nu, t) &= -e^{-2\nu}(-2\nu^3 + 4\nu^2 + \nu - 1)t^2, \\
\eta_3(\nu, t) &= -\frac{\nu e^{-2\nu}(2\nu^3 - 6\nu^2 + 3)t^3}{3}, \\
&\vdots \\
\eta_k(\nu, t) &= \frac{4(-1)^k t^k \nu^{k-2} e^{-2\nu}}{k!}\left(\nu^3 - k\nu^2 + \frac{k(k-3)}{4}\nu + \frac{k(k-1)}{4}\right).
\end{aligned}$$

Hence, the TSS consisting of n terms is expressed as

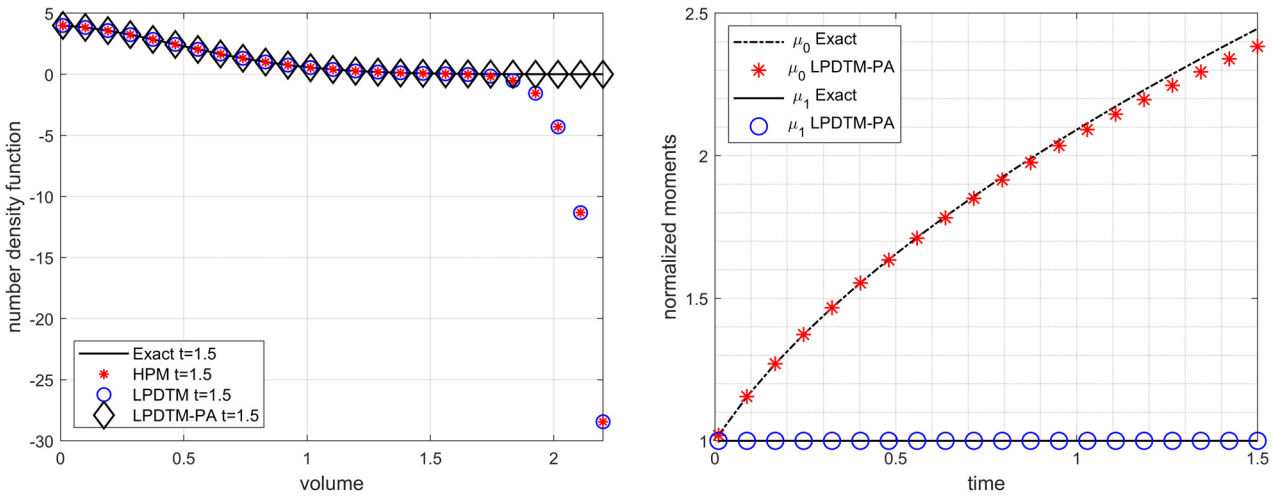

(a) Number density function (b) Normalized moments

FIG. 2. Comparison of number density function and moments for $B(\nu, y) = 2(\nu + y)$ with IC $\eta(\nu, 0) = e^{-\nu}$: (a) number density function and (b) normalized moments.

$$\Psi_n(\nu,t) = \sum_{k=0}^{n} \frac{4(-1)^k t^k \nu^{k-2} e^{-2\nu}}{k!} (\nu^3 - k\nu^2 + \frac{k(k-3)}{4}\nu + \frac{k(k-1)}{4}). \tag{40}$$

By letting $n \to \infty$ in Eq. (40), we can attain the closed-form solution, which is provided as follows:

$$\eta(\nu,t) = \sum_{k=0}^{\infty} \frac{4(-1)^k t^k \nu^{k-2} e^{-2\nu}}{k!} \left(\nu^3 - k\nu^2 + \frac{k(k-3)}{4}\nu + \frac{k(k-1)}{4}\right) \to e^{-(2+t)\nu}(2+t)(t+2\nu+t\nu). \tag{41}$$

It is evident that the LPDTM tends to capture the closed-form solution of the number density function for the breakage kernel $B(\nu, y) = 2$ corresponding to the gamma initial distribution. However, to validate this result, the number density function and its integral moments are compared with FVM[60] results in Fig. 3. Figure 3(a) illustrates that the solutions initially deviate. This discrepancy arises because the FVM requires a large number of cells to accurately capture the number density function. As depicted in Fig. 3(b), increasing the number of cells notably enhances the quality of the solutions but at a computational cost. Moreover, the zeroth and first order moments show high accuracy and match well with the FVM as shown in Figs. 3(c) and 3(d), respectively.

TABLE II. Relative errors in the number density function obtained using $B(\nu, y) = 2(\nu + y)$ with $\eta(\nu, 0) = e^{-\nu}$.

k	Pade Order	HPM	LPDTM-PA
6	[3,3]	8.6251×10^{-3}	4.5065×10^{-5}
8	[4,4]	2.9284×10^{-3}	2.2103×10^{-6}
10	[5,5]	7.6830×10^{-4}	9.9206×10^{-8}
12	[6,6]	1.5409×10^{-4}	3.8716×10^{-9}

2. $B(\nu,y)=2(\nu+y)$ with an initial distribution $\eta(\nu,0)=4\nu e^{-2\nu}$

For this case also, the analytical solution of the number density function is not available in the literature. The series component from Eq. (12) is obtained as

$$\begin{aligned}
\eta_0(\nu,t) &= 4\,\nu\, e^{-2\nu},\\
\eta_1(\nu,t) &= 2\, e^{-2\nu}(-2\,\nu^3 + 2\,\nu^2 + 2\,\nu + 1)t,\\
\eta_2(\nu,t) &= -2\,\nu^2\, e^{-2\nu}(-\nu^3 + 2\,\nu^2 + 2\,\nu + 1)t^2,\\
\eta_3(\nu,t) &= \frac{\nu^4\, e^{-2\nu}(-2\,\nu^3 + 6\,\nu^2 + 6\,\nu + 3)t^3}{3},\\
&\vdots\\
\eta_k(\nu,t) &= \frac{4(-1)^k t^k \nu^{2k-2} e^{-2\nu}}{k!}\left(\nu^3 - k\nu^2 - k\nu - \frac{k}{2}\right).
\end{aligned}$$

Therefore, the TSS consisting of n terms is expressed as

$$\Psi_n(\nu,t) = \sum_{k=0}^{n} \frac{4(-1)^k t^k \nu^{2k-2} e^{-2\nu}}{k!}\left(\nu^3 - k\nu^2 - k\nu - \frac{k}{2}\right). \tag{42}$$

As $n \to \infty$, the closed-form solution is obtained as follows:

$$\eta(\nu,t) = \sum_{k=0}^{\infty} \frac{4(-1)^k t^k \nu^{2k-2} e^{-2\nu}}{k!}\left(\nu^3 - k\nu^2 - k\nu - \frac{k}{2}\right) \to 2e^{-(2+t\nu)\nu}(2+t)(t+2\nu+2t\nu+2t\nu^2). \tag{43}$$

Analogous to previous cases, the proposed approach obtained the new closed-form solution, which is not available in the literature. The comparison of different results obtained using the proposed approach against the FVM is shown in Fig. 4. As shown in Figs. 4(a) and 4(b), the results obtained for the number density functions using the coupled LPDTM approach overlap with the FVM solutions. In addition, the integral zeroth and first order moments estimated from the number density functions are shown in Figs. 4(c) and 4(d).

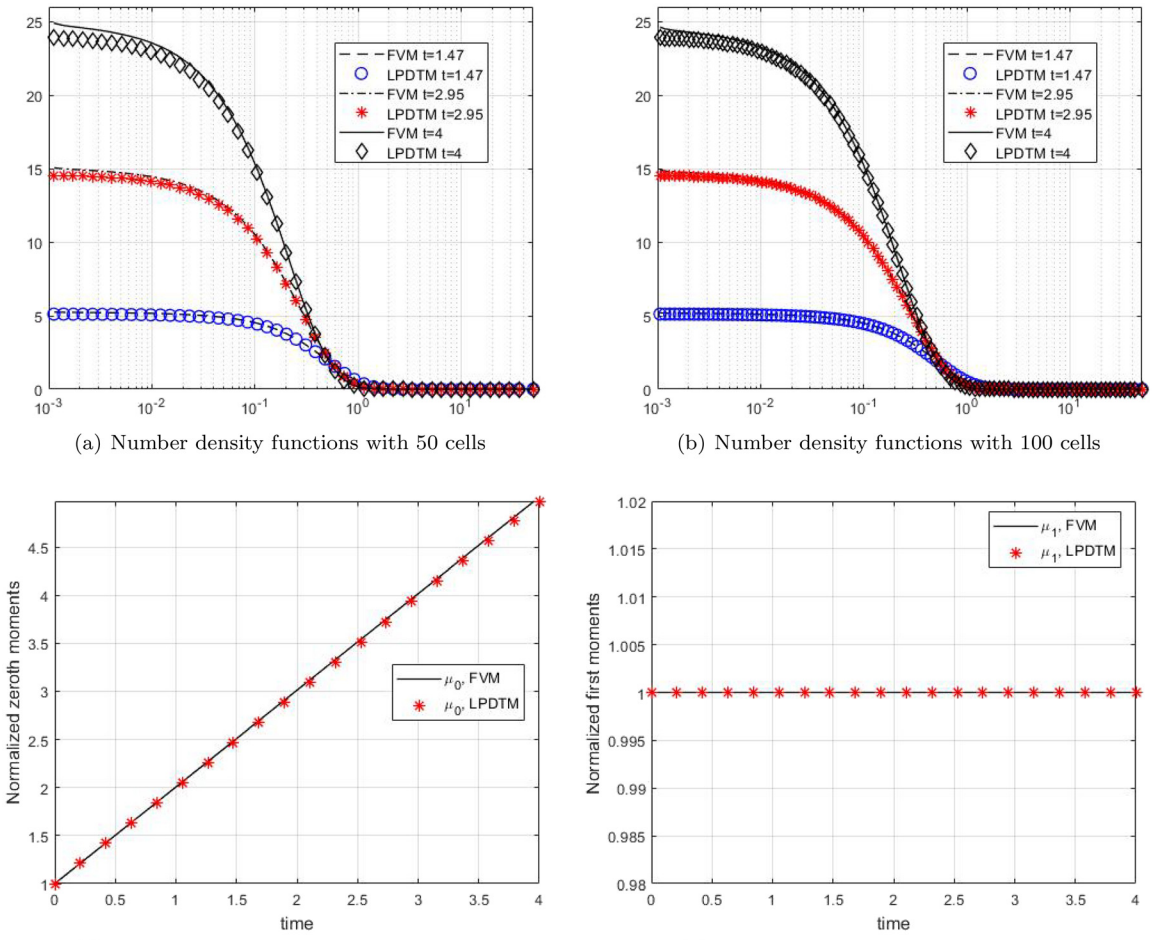

(a) Number density functions with 50 cells

(b) Number density functions with 100 cells

(c) Normalized zeroth moment with 50 cells

(d) Normalized first moment with 50 cells

FIG. 3. Comparison of number density functions and moments for $B(\nu, y) = 2$ with $\eta(\nu, 0) = 4\nu e^{-2\nu}$: (a) number density function with 50 cells, (b) number density function with 100 cells, (c) normalized zeroth moments with 50 cells, and (d) normalized first moment with 50 cells.

3. $B(v, y) = \frac{2}{\sqrt{v}+y}$ with an initial distribution $\eta(v, 0) = 4ve^{-2v}$

For showing the applicability of the proposed approach, a more complex fragmentation kernel $B(\nu, y) = \frac{2}{\sqrt{\nu}+y}$ is considered corresponding to a gamma distribution $\eta(\nu, 0) = 4\nu e^{-2\nu}$. By following the same procedure, we calculated few components of the series solution given by

$$\eta_0(\nu, t) = 4\nu e^{-2\nu},$$

$$\eta_1(\nu, t) = \frac{t\left(\sqrt{2\pi}\nu\,\mathrm{erfc}\left(\sqrt{2}\sqrt{\nu}\right) + 4e^{-2\nu}\nu^{3/2} - 4e^{-2\nu}\nu^{5/2}\right)}{\nu},$$

$$\eta_2(\nu, t) = -5\sqrt{\frac{\pi}{2}}t^2\sqrt{\nu}\,\mathrm{erfc}\left(\sqrt{2}\sqrt{\nu}\right) + 2t^2e^{-2\nu}\nu^2 + 3t^2e^{-2\nu} - 4t^2e^{-2\nu}\nu,$$

$$\eta_3(\nu, t) = 5\sqrt{\frac{\pi}{2}}t^3\nu\,\mathrm{erfc}\left(\sqrt{2}\sqrt{\nu}\right) + \frac{3}{4}\sqrt{\frac{\pi}{2}}t^3\,\mathrm{erfc}\left(\sqrt{2}\sqrt{\nu}\right) + 2t^3e^{-2\nu}\nu^{3/2} - \frac{2}{3}t^3e^{-2\nu}\nu^{5/2} - \frac{7}{2}t^3e^{-2\nu}\sqrt{\nu},$$

and so on. Here, $\mathrm{erfc}(\nu)$ defines the complementary error function for $\nu \geq 0$. It can be seen that the complexity of the series solutions is quite higher compared to previous cases. So finding the closed-form solution for this case is not possible. Hence, the quality of the solution is assessed by implementing the Padé approximant on the TSS. The TSS using eight components is obtained as

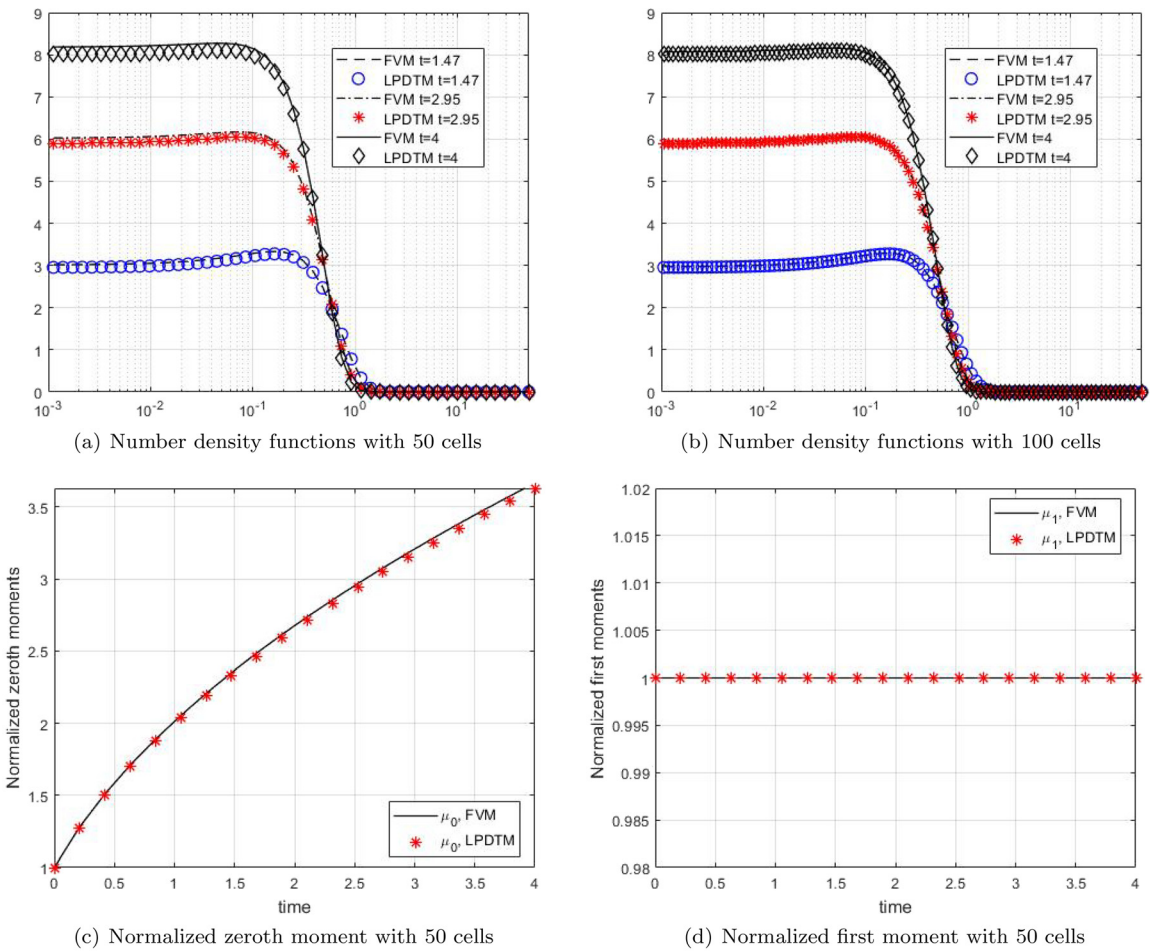

(a) Number density functions with 50 cells

(b) Number density functions with 100 cells

(c) Normalized zeroth moment with 50 cells

(d) Normalized first moment with 50 cells

FIG. 4. Comparison of number density functions and moments for $B(\nu, y) = 2(\nu + y)$ with $\eta(\nu, 0) = 4\nu e^{-2\nu}$: (a) number density function with 50 cells, (b) number density function with 100 cells, (c) normalized zeroth moment with 50 cells, and (d) normalized first moment with 50 cells.

$$
\begin{aligned}
\Psi_8(\nu,t) = &-\frac{1}{72}e^{-2\nu}t^7\nu^{3/2} - \frac{19}{24}e^{-2\nu}t^5\nu^{3/2} + 2e^{-2\nu}t^3\nu^{3/2} - \frac{7}{32}\sqrt{\frac{\pi}{2}}t^6\,\mathrm{erfc}\left(\sqrt{2}\sqrt{\nu}\right)\nu^{3/2} - \frac{35}{12}\sqrt{\frac{\pi}{2}}t^4\,\mathrm{erfc}\left(\sqrt{2}\sqrt{\nu}\right)\nu^{3/2} - \frac{19}{360}e^{-2\nu}t^7\nu^{5/2} \\
&+ \frac{1}{6}e^{-2\nu}t^5\nu^{5/2} - \frac{2}{3}e^{-2\nu}t^3\nu^{5/2} - \frac{9}{640}\sqrt{\frac{\pi}{2}}t^8\,\mathrm{erfc}\left(\sqrt{2}\sqrt{\nu}\right)\nu^{5/2} - \frac{7}{20}\sqrt{\frac{\pi}{2}}t^6\,\mathrm{erfc}\left(\sqrt{2}\sqrt{\nu}\right)\nu^{5/2} + \frac{1}{180}e^{-2\nu}t^7\nu^{7/2} - \frac{1}{30}e^{-2\nu}t^5\nu^{7/2} \\
&- \frac{11}{672}\sqrt{\frac{\pi}{2}}t^8\,\mathrm{erfc}\left(\sqrt{2}\sqrt{\nu}\right)\nu^{7/2} - \frac{e^{-2\nu}t^7\nu^{9/2}}{1260} + \frac{e^{-2\nu}t^8\nu^5}{10\,080} + \frac{1}{180}e^{-2\nu}t^6\nu^4 - \frac{e^{-2\nu}t^8\nu^4}{1260} + \frac{29e^{-2\nu}t^8\nu^3}{2880} - \frac{1}{30}e^{-2\nu}t^6\nu^3 + \frac{1}{6}e^{-2\nu}t^4\nu^3 \\
&+ \frac{1}{12}t^7\,\mathrm{erfc}\left(\sqrt{2}\sqrt{\nu}\right)\sqrt{\frac{\pi}{2}}\nu^3 + \frac{1}{288}e^{-2\nu}t^8\nu^2 + \frac{11}{48}e^{-2\nu}t^6\nu^2 - \frac{2}{3}e^{-2\nu}t^4\nu^2 + 2e^{-2\nu}t^2\nu^2 + \frac{1}{16}t^7\,\mathrm{erfc}\left(\sqrt{2}\sqrt{\nu}\right)\sqrt{\frac{\pi}{2}}\nu^2 \\
&+ \frac{7}{6}t^5\,\mathrm{erfc}\left(\sqrt{2}\sqrt{\nu}\right)\sqrt{\frac{\pi}{2}}\nu^2 + 4e^{-2\nu}\nu + \frac{1}{24}e^{-2\nu}t^6\nu + \frac{49}{24}e^{-2\nu}t^4\nu - 4e^{-2\nu}t^2\nu + \frac{9}{16}t^5\,\mathrm{erfc}\left(\sqrt{2}\sqrt{\nu}\right)\sqrt{\frac{\pi}{2}}\nu \\
&+ 5t^3\,\mathrm{erfc}\left(\sqrt{2}\sqrt{\nu}\right)\sqrt{\frac{\pi}{2}}\nu + \frac{1}{12}e^{-2\nu}t^4 + 3e^{-2\nu}t^2 - \frac{15}{16}\sqrt{\frac{\pi}{2}}t^4\sqrt{\nu}\,\mathrm{erfc}\left(\sqrt{2}\sqrt{\nu}\right) - 5\sqrt{\frac{\pi}{2}}t^2\sqrt{\nu}\,\mathrm{erfc}\left(\sqrt{2}\sqrt{\nu}\right) \\
&+ \frac{3}{4}t^3\,\mathrm{erfc}\left(\sqrt{2}\sqrt{\nu}\right)\sqrt{\frac{\pi}{2}} - \frac{1}{12}e^{-2\nu}t^5\sqrt{\nu} - \frac{7}{2}e^{-2\nu}t^3\sqrt{\nu} + \frac{t\left(4e^{-2\nu}\nu^{3/2} - 4e^{-2\nu}\nu^{5/2} + \mathrm{erfc}\left(\sqrt{2}\sqrt{\nu}\right)\sqrt{2\pi\nu}\right)}{\nu}.
\end{aligned}
\tag{44}
$$

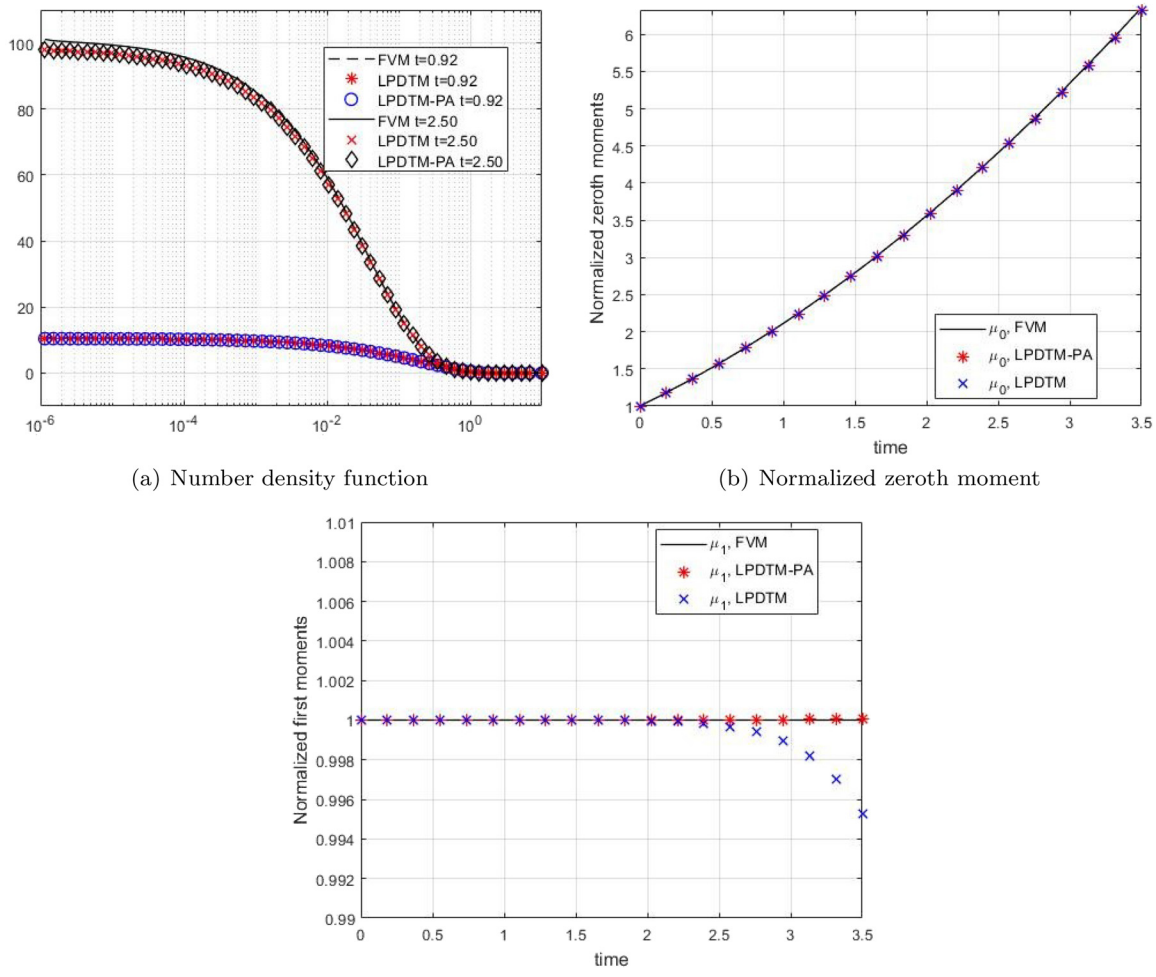

(a) Number density function

(b) Normalized zeroth moment

(c) Normalized first moment

FIG. 5. Comparison of number density function and moments for $B(\nu, y) = \frac{2}{\sqrt{\nu+y}}$ with $\eta(\nu, 0) = 4\nu e^{-2\nu}$: (a) number density function, (b) normalized zeroth moment, and (c) normalized first moment.

The above-mentioned series solution of the number density functions captures well by both LPDTM and LPDTM-PA as shown in Fig. 5(a). LPDTM captures zeroth moment with high accuracy and matches well with the FVM results as shown in Fig. 5(b); however, its first order moment shows deviation from the FVM solutions as shown in Fig. 5(c), that is, the total volume in the system is lost. The conservation of the total volume is the most important criteria for any numerical and analytical methods. Therefore, in order to achieve this, an $[4, 4]$ order Padé approximant is employed on the truncated series solution (44) with respect to variable t. It can be observed from Fig. 5 that the coupled LPDTM and Padé approximant approach not only predicts the number density function accurately but also integral zeroth and first moments with high precision and overlaps with the FVM results.

4. $B(\nu, y) = 2$ with an initial distribution $\eta(\nu, 0) = \nu e^{-\nu}$

Next, the fragmentation kernel $B(\nu, y) = 2$ is considered with an initial distribution $\eta(\nu, 0) = \nu e^{-\nu}$. For this case also, the analytical solution of the number density function is not available in the literature. Using the expression of LPDTM (12), the components of the series are obtained as

$$\eta_0(\nu, t) = \nu e^{-\nu},$$
$$\eta_1(\nu, t) = e^{-\nu}(-\nu^2 + 2\nu + 2)t,$$
$$\eta_2(\nu, t) = -\frac{e^{-\nu}(-\nu^3 + 4\nu^2 + 2\nu - 4)t^2}{2},$$
$$\eta_3(\nu, t) = -\frac{\nu e^{-\nu}(\nu^3 - 6\nu^2 + 12)t^3}{6},$$
$$\vdots$$
$$\eta_k(\nu, t) = \frac{4(-1)^k t^k \nu^{k-2} e^{-\nu}}{k!}(\nu^3 - 2k\nu^2 + k(k-3)\nu + 2k(k-1)).$$

Similarly, as above, the TSS using n terms is given by

$$\Psi_n(\nu,t)=\frac{4(-1)^k t^k \nu^{k-2} e^{-\nu}}{k!}(\nu^3-2k\nu^2+k(k-3)\nu+2k(k-1)). \tag{45}$$

As $n\to\infty$, the closed-form solution is obtained as follows:

$$\eta(\nu,t)=\sum_{k=0}^{\infty}\frac{4(-1)^k t^k \nu^{k-2} e^{-\nu}}{k!}(\nu^3-2k\nu^2+k(k-3)\nu+2k(k-1)) \to e^{-(1+t)\nu}(2+t)(2t+2t^2+\nu+2t\nu+t^2\nu). \tag{46}$$

Once again, it is demonstrated that the proposed approach has obtained a new closed-form solution that does not exist in the literature. Figure 6 shows the comparison of the series solutions of the number density function and integral moments obtained using the LPDTM with the FVM results. The number density function estimated by the proposed method is matching well with FVM (with various numbers of cell) as depicted in Figs. 6(a) and 6(b). In addition, the zeroth and first order moments predicted very well by the proposed method [refer to Figs. 6(c) and 6(d)].

V. CONCLUDING REMARKS AND FUTURE PROSPECT

In this study, an efficient semi-analytical coupled approach based on the Laplace projected differential transform and Padé approximant for approximating the hyperbolic fragmentation equation has been presented. The mathematical derivation of the method has been supported by conducting a rigorous convergence analysis employing the concept of Banach contraction principle. Most importantly, the new approach obtained the closed-form solutions of the number density corresponding to different breakage kernels and initial conditions. In cases where closed-form solutions were not obtained, it has been demonstrated that the utilization of the Padé approximant significantly enhances the accuracy of the obtained truncated series solution. This coupled approach offered numerous benefits, notably capturing accurate results over an extended time domain while requiring only a few number of series terms. This is particularly beneficial given the challenges posed by the presence of dependent double integrals and complex kernels within the fragmentation equation. For the complex structured kernel discussed in Sec. IV B 3, obtaining explicit solutions

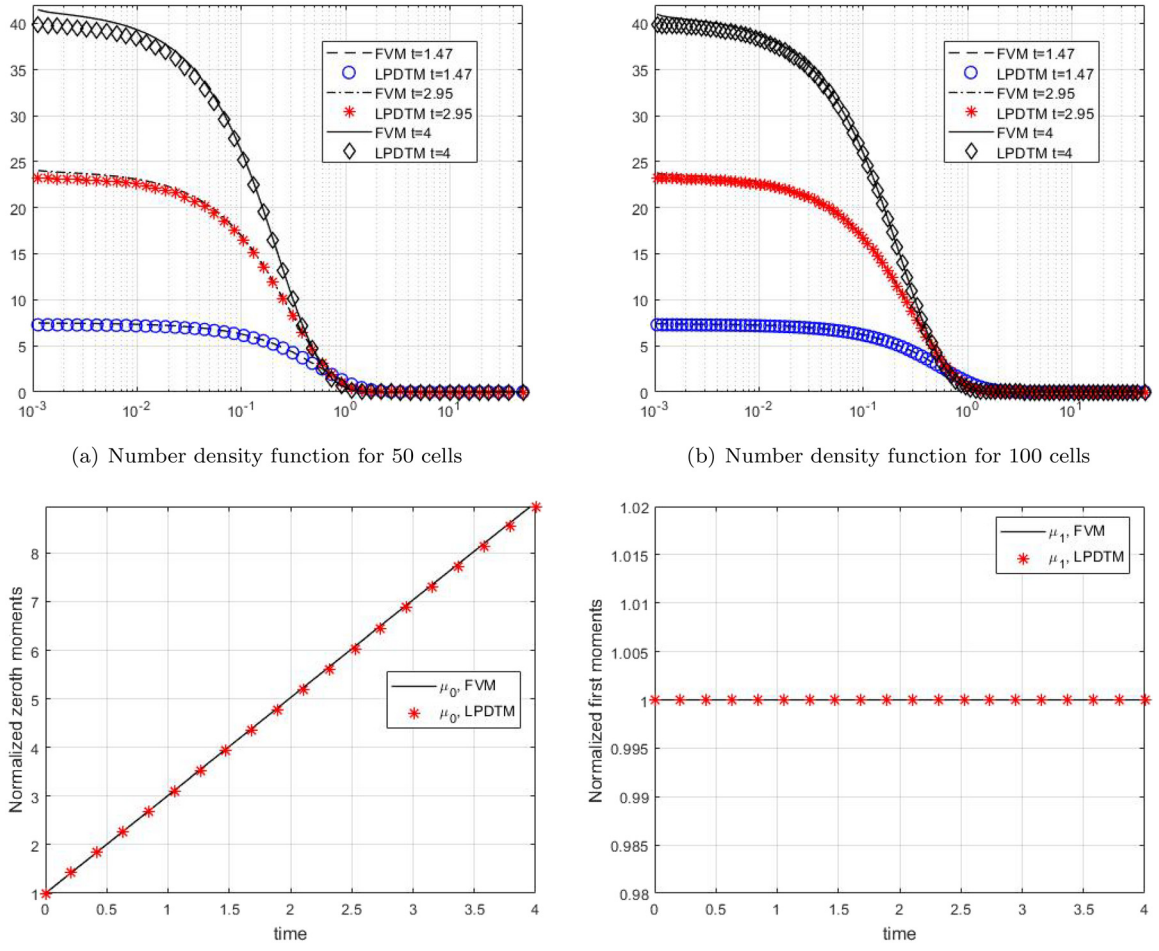

(a) Number density function for 50 cells

(b) Number density function for 100 cells

(c) Normalized zeroth moment for 50 cells

(d) Normalized first moment for 50 cells

FIG. 6. Comparison of number density functions and moments for $B(\nu,y)=2$ with $\eta(\nu,0)=\nu e^{-\nu}$: (a) number density function with 50 cells, (b) number density function with 100 cells, (c) normalized zeroth moment with 50 cells, and (d) normalized first moment with 50 cells.

for the number density functions is challenging due to the presence of error functions within the series terms. Through comparative analysis of relative errors in the number density functions, it has been demonstrated that the coupled approach outperforms the existing homotopy perturbation method.[15] Based on the findings of this study, it can be concluded that the proposed method represents a robust and generic approach for solving the classical hyperbolic fragmentation population balance equation.

In future, due to high efficiency and accuracy, the current approach will be extended to solve a nonlinear collisional fragmentation equation.[61,62] In addition, the proposed approach will also be extended to approximate multidimensional fragmentation and aggregation equations.[28,63,64]

ACKNOWLEDGMENTS

The authors did not receive support from any organization for the submitted work.

AUTHOR DECLARATIONS

Conflict of Interest

The authors have no conflicts to disclose.

Author Contributions

Nisha Yadav and Zeeshan Ansari contributed equally to this work.

Nisha Yadav: Conceptualization (equal); Data curation (equal); Formal analysis (equal); Investigation (equal); Methodology (equal); Software (equal); Validation (equal); Visualization (equal); Writing – original draft (equal). **Zeeshan Ansari:** Conceptualization (equal); Data curation (equal); Formal analysis (equal); Investigation (equal); Methodology (equal); Resources (equal); Validation (equal); Writing – original draft (equal). **Randhir Singh:** Formal analysis (equal); Methodology (equal); Validation (equal). **Ashok Das:** Formal analysis (equal); Resources (equal); Validation (equal); Writing – original draft (equal); Writing – review & editing (equal). **Sukhjit Singh:** Formal analysis (equal); Methodology (equal); Supervision (equal); Writing – original draft (equal); Writing – review & editing (equal). **Stefan Heinrich:** Formal analysis (equal); Supervision (equal); Validation (equal); Writing – review & editing (equal). **Mehakpreet Singh:** Conceptualization (equal); Formal analysis (equal); Investigation (equal); Methodology (equal); Project administration (equal); Software (equal); Supervision (equal); Validation (equal); Visualization (equal); Writing – original draft (equal); Writing – review & editing (equal).

DATA AVAILABILITY

Data sharing is not applicable to this article as no new data were created or analyzed in this study.

APPENDIX: BANACH SPACE

Theorem A.1. *The space $\mathcal{B}$ along with the norm $||\eta||_{\mathcal{B}}$ is a Banach space.*

Proof. To demonstrate that $\mathcal{B}$ is a Banach space, we must show that every Cauchy sequence in $\mathcal{B}$ converges to an element within $\mathcal{B}$.

Let η_k be a Cauchy sequence in $\mathcal{B}$. By the definition of $\mathcal{B}$, we have that $(1+\nu)\eta_k := w_k$ is a Cauchy sequence in $L^1(0,\infty)$, but $L^1(0,\infty)$ is a Banach space; therefore,

$$w_k \to w \quad \text{in} \quad L^1(0,\infty). \tag{A1}$$

Now, define $\eta := (1+\nu)^{-1} w$ and we show that η is in $L^1(0,\infty)$. As $w \in L^1(0,\infty)$, we have

$$\begin{aligned} ||\eta||_{\mathcal{B}} &= \sup_{t\in[0,T]} \int_0^\infty (1+\nu)|\eta|\, d\nu \\ &= \sup_{t\in[0,T]} \int_0^\infty (1+\nu)(1+\nu)^{-1}|w|\, d\nu < \infty. \end{aligned} \tag{A2}$$

By using $\int |ab| \le ||a||_\infty ||b||_{L^1}$, we have

$$\int_0^\infty |\eta|\, d\nu = \int_0^\infty (1+\nu)^{-1}|w|\, d\nu \le ||(1+\nu)^{-1}||_\infty ||w||_{L^1} < \infty. \tag{A3}$$

Thus, we have $\eta \in \mathcal{B}$. Now,

$$\begin{aligned} ||\eta_k - \eta||_{\mathcal{B}} &= \sup_{t\in[0,T]} \int_0^\infty (1+\nu)|\eta_k - \eta|\, d\nu \\ &= \sup_{t\in[0,T]} \int_0^\infty |w_k - w|\, d\nu \to 0 \quad \text{as} \quad k \to \infty. \end{aligned} \tag{A4}$$

Hence, every Cauchy sequence in $\mathcal{B}$ converges to an element in $\mathcal{B}$. □

REFERENCES

[1]M. Jie, W. Ze-Teng, Y. Yu-Cheng, and L. Dongyue, "Numerical treatments for large eddy simulations of liquid–liquid dispersions via population balance equation," Phys. Fluids **35**(6), 063334 (2023).
[2]Q. Wang, B. Wang, C. Wan, H. Zhang, and Y. Liu, "Modeling the distribution characteristics of vapor bubbles in cavitating flows," Phys. Fluids **35**(12), 123316 (2023).
[3]A. Rahimzadeh, F. Ein-Mozaffari, and A. Lohi, "Influence of rheological parameters on the performance of the aerated coaxial mixer containing a pseudoplastic fluid," Phys. Fluids **36**(5), 053102 (2024).
[4]Y. K. Ho, C. Kirse, H. Briesen, M. Singh, C.-H. Chan, and K.-W. Kow, "Towards improved predictions for the enzymatic chain-end scission of natural polymers by population balances: The need for a non-classical rate kernel," Chem. Eng. Sci. **176**, 329–342 (2018).
[5]M. Li, A. Li, J. Zhang, Y. Huang, and J. Li, "Effects of particle sizes on compressive deformation and particle breakage of gangue used for coal mine goaf backfill," Powder Technol. **360**, 493–502 (2020).
[6]P. Semsari Parapari, M. Parian, and J. Rosenkranz, "Breakage process of mineral processing comminution machines—An approach to liberation," Adv. Powder Technol. **31**(9), 3669–3685 (2020).
[7]A. Das, J.-S. Kroll-Rabotin, T. Quatravaux, and J.-P. Bellot, "Investigating chemical heterogeneity in inclusion populations: A multivariate population balance model study in gas-stirred ladles," Ind. Eng. Chem. Res. **62**(48), 20789–20801 (2023).
[8]K. Albion, L. Briens, C. Briens, and F. Berruti, "Detection of the breakage of pharmaceutical tablets in pneumatic transport," Int. J. Pharm. **322**(1–2), 119–129 (2006).
[9]A. Das, S. Bhoi, D. Sarkar, and J. Kumar, "Sonofragmentation of rectangular plate-like crystals: Bivariate population balance modeling and experimental validation," Cryst. Growth Des. **20**(8), 5424–5434 (2020).
[10]A. Maharana, A. Das, J. Kumar, and D. Sarkar, "Multivariate population balance modeling and simulation of ultrasound-assisted crystallization of a plate-

type pharmaceutical: Nucleation, growth, and breakage," Comput. Chem. Eng. **184**, 108651 (2024).
[11]M. Peglow, J. Kumar, and L. Mörl, "Investigation of coalescence kinetics of microcristalline cellulose in fluidised bed spray agglomeration: Experimental studies and modelling approach," Braz. J. Chem. Eng. **22**, 165–172 (2005).
[12]H. Liu and M. Li, "Two-compartmental population balance modeling of a pulsed spray fluidized bed granulation based on computational fluid dynamics (CFD) analysis," Int. J. Pharm. **475**(1–2), 256–269 (2014).
[13]S. Wang, N. Galanos, A. Rousset, K. Buffet, S. Cecioni, D. Lafont, S. P. Vincent, and S. Vidal, "Fucosylation of triethyleneglycol-based acceptors into 'clickable'α-fucosides," Carbohydr. Res. **395**, 15–18 (2014).
[14]A. Zaccone, A. Gäbler, S. Maaß, D. Marchisio, and M. Kraume, "Drop breakage in liquid–liquid stirred dispersions: Modelling of single drop breakage," Chem. Eng. Sci. **62**(22), 6297–6307 (2007).
[15]P. Kushwah, A. Paswan, V. Thota, J. Saha, M. Singh, and K. Moroney, "New semi-analytical approach and its convergence analysis for a classical hyperbolic fragmentation model: A homotopy perturbation method," J. Comput. Sci. **73**, 102135 (2023).
[16]J.-P. Bourgade and F. Filbet, "Convergence of a finite volume scheme for coagulation-fragmentation equations," Math. Comput. **77**(262), 851–882 (2008).
[17]M. Singh, J. Kumar, and A. Bück, "A volume conserving discrete formulation of aggregation population balance equations on non-uniform meshes," IFAC-PapersOnLine **48**(1), 192–197 (2015).
[18]H. Y. Ismail, M. Singh, S. Shirazian, A. B. Albadarin, and G. M. Walker, "Development of high-performance hybrid ANN-finite volume scheme (ANN-FVS) for simulation of pharmaceutical continuous granulation," Chem. Eng. Res. Des. **163**, 320–326 (2020).
[19]M. Singh and G. Walker, "New discrete formulation for reduced population balance equation: An illustration to crystallization," Pharm. Res. **39**(9), 2049–2063 (2022).
[20]S. Yadav, A. Das, S. Singh, S. Tomar, R. Singh, and M. Singh, "Coupled approach and its convergence analysis for aggregation and breakage models: Study of extended temporal behaviour," Powder Technol. **439**, 119714 (2024).
[21]R. M. Ziff and E. D. McGrady, "The kinetics of cluster fragmentation and depolymerisation," J. Phys. A **18**(15), 3027 (1985).
[22]D. L. Marchisio and R. O. Fox, "Solution of population balance equations using the direct quadrature method of moments," J. Aerosol Sci. **36**(1), 43–73 (2005).
[23]P. L. C. Lage, "On the representation of QMOM as a weighted-residual method—The dual-quadrature method of generalized moments," Comput. Chem. Eng. **35**(11), 2186–2203 (2011).
[24]J. Kumar, M. Peglow, G. Warnecke, S. Heinrich, and L. Mörl, "Improved accuracy and convergence of discretized population balance for aggregation: The cell average technique," Chem. Eng. Sci. **61**(10), 3327–3342 (2006).
[25]M. Singh, T. Matsoukas, A. B. Albadarin, and G. Walker, "New volume consistent approximation for binary breakage population balance equation and its convergence analysis," ESAIM **53**(5), 1695–1713 (2019).
[26]A. Das, J. Kumar, M. Dosta, and S. Heinrich, "On the approximate solution and modeling of the kernel of nonlinear breakage population balance equation," SIAM J. Sci. Comput. **42**(6), B1570–B1598 (2020).
[27]M. Singh and G. Walker, "Finite volume approach for fragmentation equation and its mathematical analysis," Numer. Algor. **89**(2), 465–486 (2022).
[28]M. Singh, T. Matsoukas, V. Ranade, and G. Walker, "Discrete finite volume formulation for multidimensional fragmentation equation and its convergence analysis," J. Comput. Phys. **464**, 111368 (2022).
[29]J. Paul, A. Das, and J. Kumar, "Moments preserving finite volume approximations for the non-linear collisional fragmentation model," Appl. Math. Comput. **436**, 127494 (2023).
[30]Z. Ansari, M. Rae, and M. Singh, "Two moments preserving sectional approach for an enzymatic coagulation equation," Phys. Fluids **36**(6), 067112 (2024).
[31]R. Gunawan, I. Fusman, and R. D. Braatz, "High resolution algorithms for multidimensional population balance equations," AIChE J. **50**(11), 2738–2749 (2004).
[32]D. T. Robson, A. C. W. Baas, and A. Annibale, "A combined model of aggregation, fragmentation, and exchange processes: Insights from analytical calculations," J. Stat. Mech. **2021**, 053203.
[33]M. Singh, S. Shirazian, V. Ranade, G. M. Walker, and A. Kumar, "Challenges and opportunities in modelling wet granulation in pharmaceutical industry—A critical review," Powder Technol. **403**, 117380 (2022).
[34]M. Singh, V. Ranade, O. Shardt, and T. Matsoukas, "Challenges and opportunities concerning numerical solutions for population balances: A critical review," J. Phys. A **55**(38), 383002 (2022).
[35]R. M. Ziff, "New solutions to the fragmentation equation," J. Phys. A **24**(12), 2821 (1991).
[36]Z. Cheng and S. Redner, "Scaling theory of fragmentation," Phys. Rev. Lett. **60**(24), 2450 (1988).
[37]M. Kostoglou and A. J. Karabelas, "A study of the nonlinear breakage equation: Analytical and asymptotic solutions," J. Phys. A **33**(6), 1221 (2000).
[38]Z. Cheng and S. Redner, "Kinetics of fragmentation," J. Phys. A **23**(7), 1233 (1990).
[39]R. Singh, J. Saha, and J. Kumar, "Adomian decomposition method for solving fragmentation and aggregation population balance equations," J. Appl. Math. Comput. **48**, 265–292 (2015).
[40]G. Kaur, R. Singh, M. Singh, J. Kumar, and T. Matsoukas, "Analytical approach for solving population balances: A homotopy perturbation method," J. Phys. A **52**(38), 385201 (2019).
[41]N. Yadav, M. Singh, S. Singh, R. Singh, J. Kumar, and S. Heinrich, "An efficient approach to obtain analytical solution of nonlinear particle aggregation equation for longer time domains," Adv. Powder Technol. **35**(3), 104370 (2024).
[42]S. Yadav, S. Keshav, S. Singh, M. Singh, and J. Kumar, "Homotopy analysis method and its convergence analysis for a nonlinear simultaneous aggregation-fragmentation model," Chaos, Solitons Fractals **177**, 114204 (2023).
[43]N. Yadav, M. Singh, S. Singh, R. Singh, and J. Kumar, "A note on homotopy perturbation approach for nonlinear coagulation equation to improve series solutions for longer times," Chaos, Solitons Fractals **173**, 113628 (2023).
[44]J. K. Zhou, *Differential Transformation and Its Applications for Electronic Circuits* (Huazhong Science and Technology University Press, China, 1986).
[45]C.-L. Chen and Y. C. Liu, "Solution of two-point boundary-value problems using the differential transformation method," J. Optim. Theory Appl. **99**, 23–35 (1998).
[46]A.-M. Batiha and B. Batiha, "Differential transformation method for a reliable treatment of the nonlinear biochemical reaction model," Adv. Stud. Biol. **3**(8), 355–360 (2011).
[47]F. Ayaz, "Applications of differential transform method to differential-algebraic equations," Appl. Math. Comput. **152**(3), 649–657 (2004).
[48]A. S. V. Ravi Kanth and K. Aruna, "Two-dimensional differential transform method for solving linear and non-linear schrödinger equations," Chaos, Solitons Fractals **41**(5), 2277–2281 (2009).
[49]S. Momani, Z. Odibat, and V. S. Erturk, "Generalized differential transform method for solving a space-and time-fractional diffusion-wave equation," Phys. Lett. A **370**(5–6), 379–387 (2007).
[50]V. S. Erturk, S. Momani, and Z. Odibat, "Application of generalized differential transform method to multi-order fractional differential equations," Commun. Nonlinear Sci. Numer. Simul. **13**(8), 1642–1654 (2008).
[51]Z. Odibat and S. Momani, "A generalized differential transform method for linear partial differential equations of fractional order," Appl. Math. Lett. **21**(2), 194–199 (2008).
[52]B. Jang, "Solving linear and nonlinear initial value problems by the projected differential transform method," Comput. Phys. Commun. **181**(5), 848–854 (2010).
[53]K. T. Akinfe and A. C. Loyinmi, "The implementation of an improved differential transform scheme on the Schrodinger equation governing wave-particle duality in quantum physics and optics," Results Phys. **40**, 105806 (2022).
[54]B. Benhammouda, H. Vazquez-Leal, and L. Hernandez-Martinez, "Modified differential transform method for solving the model of pollution for a system of lakes," Discrete Dyn. Nat. Soc. **2014**, 645726.
[55]Z. Bekiryazici, M. Merdan, and T. Kesemen, "Modification of the random differential transformation method and its applications to compartmental models," Commun. Stat.-Theory Methods **50**(18), 4271–4292 (2021).
[56]M. M. Rashidi, "The modified differential transform method for solving MHD boundary-layer equations," Comput. Phys. Commun. **180**(11), 2210–2217 (2009).
[57]M. Mehdi Rashidi and E. Erfani, "The modified differential transform method for investigating nano boundary-layers over stretching surfaces," Int. J. Numer. Methods Heat Fluid Flow **21**(7), 864–883 (2011).
[58]C. Brezinski and J. Van Iseghem, "Padé approximations," Handbook Numer. Anal. **3**, 47–222 (1994).
[59]P. Gonnet, S. Guttel, and L. N. Trefethen, "Robust Padé approximation via SVD," SIAM Rev. **55**(1), 101–117 (2013).

[60]J. Saha, J. Kumar, and S. Heinrich, "A volume-consistent discrete formulation of particle breakage equation," Comput. Chem. Eng. **97**, 147–160 (2017).
[61]N. Yadav, A. Das, M. Singh, S. Singh, and J. Kumar, "Homotopy perturbation method and its convergence analysis for nonlinear collisional fragmentation equations," Proc. R. Soc. A **479**(2279), 20230567 (2023).
[62]A. Das, P. Kushwah, J. Saha, and M. Singh, "Improved higher-order finite volume scheme and its convergence analysis for collisional breakage equation," Appl. Numer. Math. **196**, 118–132 (2024).
[63]M. Singh, R. Singh, S. Singh, G. Walker, and T. Matsoukas, "Discrete finite volume approach for multidimensional agglomeration population balance equation on unstructured grid," Powder Technol. **376**, 229–240 (2020).
[64]S. L. Leong, M. Singh, F. Ahamed, S. Heinrich,, S. Ing Xun Tiong, I. Mei Leng Chew, and Y. Kuen Ho, "A comparative study of the fixed pivot technique and finite volume schemes for multi-dimensional breakage population balances," Adv. Powder Technol. **34**(12), 104272 (2023).